

AperTO - Archivio Istituzionale Open Access dell'Università di Torino

## Porphyrin-Loaded Pluronic Nanobubbles: A New US-Activated Agent for Future Theranostic Applications

### This is the author's manuscript

*Original Citation:*

*Availability:*

This version is available <http://hdl.handle.net/2318/1723152> since 2020-01-15T14:14:54Z

*Published version:*

DOI:10.1021/acs.bioconjchem.7b00732

*Terms of use:*

Open Access

Anyone can freely access the full text of works made available as "Open Access". Works made available under a Creative Commons license can be used according to the terms and conditions of said license. Use of all other works requires consent of the right holder (author or publisher) if not exempted from copyright protection by the applicable law.

(Article begins on next page)

# Porphyrin-Loaded Pluronic Nanobubbles: A New US-Activated Agent for Future Theranostic Applications

Federica Bosca,<sup>†</sup> Peter A. Bielecki,<sup>‡</sup> Agata A. Exner,<sup>\*,‡,§</sup> and Alessandro Barge<sup>\*,†</sup>

<sup>†</sup>Department of Drug Science and Technology, University of Turin, Via Giuria 9, 10125 Turin, Italy

<sup>‡</sup>Departments of Biomedical Engineering and <sup>§</sup>Radiology, Case Western Reserve University, 10900 Euclid Avenue, Cleveland, Ohio 44106-5056, United States

DOI: 10.1021/acs.bioconjchem.7b00732

Sonodynamic therapy (SDT)<sup>1,2</sup> is a method of cancer therapy which excites a given molecule, often a porphyrin,<sup>3</sup> through the implosion of gas bubbles arising from inertial acoustic cavitation followed by ultrasound (US) irradiation.<sup>4-6</sup> Generation of the reactive oxygen species (ROS) during the molecule's decay induces cell death, typically through the apoptotic pathway.<sup>7</sup> SDT was developed nearly two decades ago by Yumita et al.<sup>1</sup> Fundamentally, SDT is based on the photodynamic therapy (PDT) concept, but uses US as the energy source rather than light. SDT helps to overcome some PDT limitations such as PDT's low tissue penetration and longlasting skin sensitivity due to the retention of the photosensitizer in cutaneous tissue.<sup>8</sup> While the SDT mechanism remains unknown, the reported hypotheses suggest a deep link to the PDT process as molecules commonly used in PDT can also be used for SDT.

Porphyrin compounds are among the most studied species as photosensitizers because they exhibit low toxicity at therapeutic concentrations in the absence of external stimuli, in contrast to other anticancer drugs.<sup>9</sup> Moreover, porphyrins can be efficiently excited by US and they generate ROS during their decay process, inducing tumor cell death.<sup>2,10,11</sup>

Because the timing and location of US application is the key to successful SDT,<sup>12-15</sup> a technique which enables direct visualization of porphyrin delivery to the region of interest, by the same energy source (US), would be of great benefit to this therapeutic approach. Microbubbles (MBs) are US contrast agents routinely utilized in clinical diagnostic imaging and are being investigated for drug delivery applications. Shell-stabilized, gas MBs provide strong ultrasound backscatter via two mechanisms: an impedance mismatch with the gas phase and oscillating in the ultrasound field, rapidly contracting and expanding in response to the pressure changes of the sound wave.<sup>16,17</sup> MBs, which are typically in the range of 1–10  $\mu\text{m}$  in diameter, typically also resonate at the 3–12 MHz frequencies widely used for diagnostic US imaging, making them several orders of magnitude more reflective than normal body tissues. Combining the echogenic properties of MBs with the therapeutic properties of porphyrins and their US-triggered activation (at different US frequency) could improve the effectiveness of SDT. However, the size of MBs may limit their biodistribution in the tumor and hinder subsequent therapy. To increase the delivery efficiency of drug to solid tumor via the enhanced permeability and retention (EPR) effect, the ideal theranostic vehicle<sup>18-20</sup> should be scaled down to the 200–400 nm range to pass through leaky tumor vasculature. Accordingly, the aim of this work was to develop a new theranostic, echogenic, porphyrin-loaded nanoparticle capable of real-time US activation, monitoring, and activity in SDT. Some prior work has investigated theranostic systems which combine the visibility of MBs with well-known anticancer drugs (such as doxorubicin<sup>21</sup>), resulting in chemosensitizing effects. In addition, a modified porphyrin-lipid conjugate has been incorporated into MBs (which were then converted into NBs via sonication) to obtain a multimodal US and photodynamic imaging probe.<sup>22,23</sup> Callan et al. exploited the MB as Rose Bengal sonosensitizer carrier and enhancer in ROS generation upon US irradiation for SDT anticancer therapy.<sup>24,25</sup> Similarly, Liu and co-workers reported that microbubbles can markedly improve the anticancer effect of DVDMS mediated sonodynamic therapy both in vitro and in vivo.<sup>26</sup> However, to the best of our knowledge, there are currently no echogenic nanosystems which combine US imaging with US activated molecules for future SDT-US imaging theranostic application.<sup>27</sup>

The development of an efficient gas core nanosystem loaded with suitable amphiphilic porphyrin derivatives for eventual theranostic application in cancer therapy is proposed herein. The foundation of this construct is a lipid, surfactant, and polyacrylamide-stabilized perfluorocarbon nanobubble (NB).<sup>21,28-31</sup> These NBs are stable<sup>32</sup> and easily modifiable, and the shell can be exploited to load drugs, prodrugs, and/or vector to build theranostic and imaging agents.<sup>33</sup> NBs were formulated and separated using a well optimized procedure,<sup>30</sup> by using a lipidic film made of DPPA (1,2-dipalmitoyl-*sn*-glycero-3-phosphate), DPPC (1,2-dipalmitoyl-*sn*-glycero-3-phosphocholine), DPPE (1,2-dipalmitoyl-*sn*-glycero-3-phosphoethanolamine) (Avanti Polar Lipids, Pelham, AL), and mPEG-DSPE (1,2-distearoyl-phosphatidylethanol-amine-methyl-polyethylene glycol conjugate-2000) (Laysan Lipids, Arab, AL). The film was hydrated with Pluronic solution (Sigma-Aldrich, Milwaukee, WI) in 0.5% Irgacure (Fisher Scientific; Pittsburgh, PA) in PBS in the presence of glycerol at 75 °C. Next, NNDEA (Polysciences, Warrington, PA) and BAC (Sigma-Aldrich, Milwaukee, WI) (2:1 weight ratio) were added, and air was removed from the sealed vials and replaced with octafluoropropane before shaking. To include porphyrin compounds in the NBs lipidic layer, by noncovalent interaction, a structural modification of this compound is required. Starting from commercial porphyrin it is possible to tune its lipophilic property by conjugation with suitable aliphatic chains. Hence, two porphyrin derivatives have been synthesized: the first class being more lipophilic and the second class more amphiphilic.

The main structural difference consists of a dioxyethylene bridge between porphyrin nucleus and the lipid chains, which confers the amphiphilic behavior to the entire molecule (Scheme 1).

Porphyrin classes were synthesized by altering reaction parameters (i.e., reactant concentrations, additives, and reaction time) to produce a porphyrin mixture with convenient distribution of mono-, di-, tri-, and tetra-substituted compounds. The optimum ratio and reaction end points were identified by HPLC-MS, as well as porphyrin isolation. The first class of lipophilic porphyrin, originated from commercially available meso-tetrakis(4-hydroxyphenyl)-porphyrin (compound 1, Scheme 1), was synthesized by a reaction with Br-dodecane in the presence of Na<sub>2</sub>CO<sub>3</sub>.

18-Crown-6-ether was added to increase the ability of sodium carbonate to behave as a base. This approach was designed to maximize the tetra-alkylated derivative to give higher yield of this compound than those obtained in already reported procedures,<sup>34</sup> allowing at the same time, to isolate significant amounts of mono-, di-, and tri-alkylated compounds. The second class of amphiphilic porphyrin, originated from commercially available meso-tetrakis(4-carboxyphenyl)-porphyrin, was synthesized by a reaction with a suitably protected diamine as per previously described procedure.<sup>35</sup> After amine deprotection, derivative 6 (Scheme 1) was reacted with lauroylchloride. The reaction conditions were optimized to obtain a mixture of mono-, bis-, tris-, and tetrakis-acylated derivatives which were separated by preparative HPLC-MS (details in SI). These isolated porphyrin derivatives were added to the NB formulation to explore the ability of these compounds to be incorporated in the lipid monolayer. NB dimension and echogenicity were evaluated.

The NB ability to load porphyrins in their lipid shell is markedly dependent on porphyrin structure. Porphyrin loading was calculated by collecting, washing, and lyophilizing the bubble layer suspension. After dissolving the residue in a mixture of methanol and chloroform (2:1), to avoid lipid aggregation, the porphyrin content was determined by fluorescence measurement. The loading of the most lipophilic structure (compound 5), was found to be very low and porphyrin was observed as nanoaggregates. A mean of 1800 porphyrin molecules were calculated for each NB. Number of porphyrin molecules per NB was derived from the overall porphyrin concentration in the bubble layer and the number of nanoparticles determined by nanoparticle tracking analysis, NTA, using the NanoSight, Malvern Instruments, as described below. Because of the lipophilic structure of compound 5, interactions with the lipid monolayer of the NB appeared unlikely. Conversely, compound 7, due to its four amphiphilic bridges (red lines in Figure 1) between the macrocyclic nucleus and the lipophilic chain (blue line in Figure 1), could be loaded more efficiently into NBs than compound 5.

An average of 3300 porphyrin molecules per NB were calculated for compound 7 and no nanoaggregates were observed. Fluorescent microscopy confirmed the distribution of compound 7 into the NB lipid monolayer.

The higher loading of compound 7 than compound 5 in the lipid NBs could be attributed to the amphiphilic nature of side chains in compound 7, which have similar structure to Pluronic L10 and to phospholipidic arrangement in the bubble shell (Figure 1).

The data suggests that porphyrin modification has to be tailored *ad hoc* to the optimized NB formulation,<sup>30</sup> mimicking the phospholipid and additive polar/hydrophobic balance and distribution. More specifically, the porphyrin chain should contain a distal lipophilic region to interact with the nonpolar phospholipid tails and Pluronic-PPO in the NB shell. The porphyrin should be amphiphilic to also allow its polar region to interact with the polar phospholipid heads and Pluronic-PEO in the NB shell. Because of porphyrin geometry, only one chain is needed to achieve successful NB incorporation; additional chains are likely not involved in the interaction with NB monolayer components.

Fluorescent microscopy supports the conclusion that compound 7 can be more efficiently incorporated into both MB and NB monolayers compared to compound 5. Due to the limits of optical resolution, colocalization of porphyrin and bubble shell via fluorescent microscopy can only be carried out on MB particles. However, it is likely that the same structure can be assumed for nanosized particles which share the same chemical composition and makeup (Figure 2a). Compound 5, which has a completely lipophilic structure, was unable to make interactions with the bubble shell and preferentially self-aggregated into nanocrystals outside the bubbles (Figure 2b).

The mean diameter and polydispersity of Pluronic nano-bubbles, which were separated from the MB population using differential centrifugation,<sup>36</sup> were measured using nanoparticle tracking analysis (NanoSight). On the basis of previously reported work,<sup>36</sup> bubbles larger than 0.7  $\mu\text{m}$  should rise a distance of 0.5 cm or greater following centrifugation at 50g for 5 min. Collecting sample below this distance ensures the presence of only NB. Without porphyrin, NB diameter was found to be  $137.0 \pm 16$  nm ( $n = 3$ ). When porphyrin was loaded into the bubble shell, the NB diameter changed to  $144.66 \pm 5.6$  nm ( $n = 3$ ) for compound 7 and  $199.5 \pm 14.6$  nm ( $n = 3$ ) for compound 5 (Figure 3a and b, respectively). Thus, when porphyrin is included in the monolayer, we can observe an increase in the overall diameter. Specifically, when the porphyrin derivative contains a “Pluronic-like” structure, as is the case with compound 7, the change in size is not so drastic as after compound 5 addition. It may be possible that Pluronic L10 is excluded from the NB structure when porphyrin molecules are included in the NB formulation, which can lead to the size increase.

If porphyrin is quite different from Pluronic L10 (compound 5), the change in diameter would be more pronounced than in the presence of a “Pluronic L10-like” porphyrin (compound 7). Thus, we can assume that the role of Pluronic can be well represented by the amphiphilic bridge because there is no significant difference in size between compound 7-loaded NB compared to unloaded NB. The concentration of NB-7 obtained from the NanoSight was  $4.13 \times 10^{11}$  ( $\pm 8.74 \times 10^9$ ) particles per mL, while the concentration of NB-5 was  $2.98 \times 10^{11}$  ( $\pm 2.59 \times 10^{10}$ ) particles per mL. The addition of compound 7 seems to lend the system itself to a more stable self-assembly of NBs.

Echogenicity of loaded NBs was evaluated and compared with unloaded NBs, which have been investigated comprehensively *in vitro* and *in vivo* in prior work.<sup>30</sup> Data obtained confirm the retained ability of this system to work as an US contrast agent after porphyrin derivative incorporation (Figure 4). Images were recovered using an Aplio XG SSA-790A clinical ultrasound imaging system (Toshiba Medical Imaging Systems, Otawara-Shi, Japan) equipped with a 12 MHz linear array transducer using a contrast harmonic imaging protocol. See SI for US set up used to image NB samples in the gel phantom. The NB stability under US irradiation, during the US image acquisition, was evaluated for both loaded and unloaded

bubbles, by measuring the decay in ultrasound signal intensity over time. These data suggest that porphyrin destabilizes the nanoconstruct reducing its signal decay rate to 25% when it is compared to unloaded NB signal (see SI for all details: the half-life of unloaded NB, under this experimental condition, is 20 min, whereas that of loaded ones is 5 min; this reduction could be related to the destabilization of the cross-linked network due to the presence of porphyrin molecules in the lipid monolayer). The sonodynamic activity was evaluated by a pilot *in vitro* test on human colon adenocarcinoma, LS 174 T cells. Cells were incubated with either unloaded NBs (reference control), 0.1 or 2.5  $\mu\text{g}/\text{mL}$  of soluble porphyrin (TPPS, *meso*-tetraphenylporphyrine-4,4',4'',4''' tetrasulfonic acid: this porphyrin shows the same macrocyclic structure, which is responsible of sonodynamic effect, of compounds 5 and 7; the only difference is in lateral chains) in the presence of unloaded NBs, or with compound 7 or 5-loaded NBs. Cells were then immediately exposed to US irradiation (no cellular uptake occurred) and, after 3 days, a proliferation test was performed. This biological analysis is aimed to compare the behavior of encapsulated porphyrin with nonencapsulated porphyrin TPPS (details in SI). Figure 5 clearly shows a statistically significant reduction in cell viability when cells were treated with NB-7, whereas no reduction was observed with unloaded NB and free, soluble TPPS.

These results could be explained considering the role of NBs as cavitation nuclei<sup>16</sup> and the distribution of porphyrin in the NB surrounding media.

When we consider the case of NB-7 and NB-5, porphyrin molecules are included in the lipidic NB shell (with different derivative content); hence, porphyrin molecules are likely very close to the cavitation implosion region. In these cases, the porphyrin excites more easily, allowing a low number of porphyrin molecules to produce a sufficient amount of ROS<sup>37,38</sup> for cell death. When porphyrin is placed outside of the NB (in the case of TPPS-nb), the collapse of bubbles excites less porphyrin molecules (which are away from the cavitation site) causing a consequently lower biological effect. It is interesting to note that there is no statistically significant difference in biological activity, upon US irradiation, between NB loaded with compound 7 or compound 5. This suggests that it is sufficient to have a very low amount of porphyrin loaded in the NB shell (1800 molecules per NB, 6 ng/mL of porphyrin) to obtain a significant effect on cell viability reduction. Porphyrin excitation is amplified by the action of gas-filled nanosystems which enhance the acoustic cavitation phenomenon.

In conclusion, this work describes a new porphyrin-loaded Pluronic NB system. The system's loading ability is notably dependent on the porphyrin structure according to the hydrophilic/lipophilic balance of the NB components. It was found that the amphiphilic compound 7 better incorporated into the NB monolayer compared to the more lipophilic compound 5. Preliminary investigation of the biological activity of porphyrin-loaded NBs on LS 174 T cells show a reduction in cell viability of over 30%. This reduction is half of that observed by Callan et al, using MB loaded with 2 orders of magnitude more concentrated Rose Bengal.<sup>24</sup> The result observed using NB loaded with low amount of compound 7 entails a marked reduction of long-lasting skin photosensitivity after treatment. Cells exposed to unloaded NBs and much higher concentrations of free, soluble porphyrin did not show a statistically significant reduction in cell viability. This phenomenon may be ascribed to the entire nanoconstruct that acts as a cavitation nucleus under US irradiation and enhance the probability of neighboring porphyrin excitation (as in the case of porphyrin loaded NBs). The addition of porphyrin compound 7 into the NB shell does not dramatically modify the NB diameter and does not induce any difference in US enhanced contrast ability compared to unloaded NBs. The advantage of this engineered nanosystem is its versatility that makes it possible to have a simultaneous real-time monitoring and porphyrin activation (by using US with different frequency), in a specific tumor area, thereby avoiding ROS production in peripheral regions. The combination of these two features gives this nanosystem promise as a theranostic agent for future applications in SDT treatment combined with diagnostic US. To the best of our knowledge, this is the first study introducing noncovalently loaded porphyrin-NBs in the SDT anticancer field.

## ASSOCIATED CONTENT

### Supporting Information

The Supporting Information is available free of charge on the ACS Publications website at DOI: 10.1021/acs.bioconjchem.7b00732.

Synthetic procedure and characterization of all synthesized porphyrin compounds (including 1D and 2D NMR spectra), NB formulation protocols and characterizations, cells culture and treatment, and *in vitro* experiment procedures (PDF)

## Corresponding Authors

\*E-mail: [agata.exner@case.edu](mailto:agata.exner@case.edu).

\*E-mail: [alessandro.barge@unito.it](mailto:alessandro.barge@unito.it).

## Notes

The authors declare no competing financial interest.

## ACKNOWLEDGMENTS

This research was supported by MIUR (fondi ricerca locale

2015) and additional support from the Case Comprehensive Cancer Center P30CA043703 in the form of a pilot grant. We would like to acknowledge Dr. Luis Solorio, PhD, for support in obtaining nanoparticle size data; Chawan Manaspon, BS, for support in *in vitro* test experiments and Christopher Hernandez, BS, for support in obtaining fluorescent microscopy data and for general suggestions.

## REFERENCES

- (1) Yumita, N., Nishigaki, R., Umemura, K., and Umemura, S. (1989) Hematoporphyrin as a Sensitizer of Cell-Damaging Effect of Ultrasound. *Jpn. J. Cancer Res.* **80**, 219–222.
- (2) Shibaguchi, H., Tsuru, H., Kuroki, M., and Kuroki, M. (2011) Sonodynamic cancer therapy: a non-invasive and repeatable approach

using low-intensity ultrasound with a sonosensitizer. *Anticancer Res.* 31,2425–2429.

(3) Hachimine, K., Shibaguchi, H., Kuroki, M., Yamada, H., Kinugasa, T., Nakae, Y., Asano, R., Sakata, I., Yamashita, Y., Shirakusa, T., et al. (2007) Sonodynamic therapy of cancer using a novel porphyrin derivative, DCPH-P-Na(I), which is devoid of photosensitivity. *Cancer Sci.* 98, 916–920.

(4) Rosenthal, I., Sostaric, J. Z., and Riesz, P. (2004) Sonodynamic therapy—a review of the synergistic effects of drugs and ultrasound. *Ultrason. Sonochem.* 11, 349–363.

(5) Tachibana, K., Feril, L. B., Jr, and Ikeda-Dantsuji, Y. (2008) Sonodynamic therapy. *Ultrasonics* 48, 253–259.

(6) ter Haar, G. (2007) Therapeutic applications of ultrasound. *Prog. Biophys. Mol. Biol.* 93, 111–129.

(7) Yumita, N., Iwase, Y., Nishi, K., Komatsu, H., Takeda, K., Onodera, K., Fukai, T., Ikeda, T., Umemura, S., Okudaira, K., et al. (2012) Involvement of reactive oxygen species in sonodynamically induced apoptosis using a novel porphyrin derivative. *Theranostics* 2, 880–888.

(8) Moriwaki, S.-I., Misawa, J., Yoshinari, Y., Yamada, I., Takigawa, M., and Tokura, Y. (2001) Analysis of photosensitivity in Japanese cancer-bearing patients receiving photodynamic therapy with porfimer sodium (Photofrin™). *Photodermatol., Photoimmunol. Photomed.* 17, 241–243.

(9) Tsuru, H., Shibaguchi, H., Kuroki, M., Yamashita, Y., and Kuroki,

M. (2012) Tumor growth inhibition by sonodynamic therapy using a novel sonosensitizer. *Free Radical Biol. Med.* 53, 464–472.

(10) Xiong, W., Wang, P., Hu, J., Jia, Y., Wu, L., Chen, X., Liu, Q., and Wang, X. (2015) A new sensitizer DVDMS combined with multiple focused ultrasound treatments: an effective antitumor strategy. *Sci. Rep.* 5, 17485.

(11) Boissenot, T., Bordat, A., Fattal, E., and Tsapis, N. (2016) Ultrasound-triggered drug delivery for cancer treatment using drug delivery systems: From theoretical considerations to practical applications. *J. Controlled Release* 241, 144–163.

(12) Lammers, T., Kiessling, F., Hennink, W. E., and Storm, G. (2010) Nanotheranostics and image-guided drug delivery: current concepts and future directions. *Mol. Pharmaceutics* 7, 1899–1912.

(13) Yuan, Y., and Liu, B. (2014) Self-assembled nanoparticles based on PEGylated conjugated polyelectrolyte and drug molecules for *Mater. Interfaces* 6, 14903–14910.

(14) Cai, W., Gao, H., Chu, C., Wang, X., Wang, J., Zhang, P., Lin, G., Li, W., Liu, G., and Chen, X. (2017) Engineering Phototheranostic Nanoscale Metal-Organic Frameworks for Multimodal Imaging- Guided Cancer Therapy. *ACS Appl. Mater. Interfaces* 9, 2040–2051.

(15) Chen, J., Ratnayaka, S., Alford, A., Kozlovskaya, V., Liu, F., Xue, B., Hoyt, K., and Kharlampieva, E. (2017) Theranostic Multilayer Capsules for Ultrasound Imaging and Guided Drug Delivery. *ACS Nano* 11, 3135–3146.

(16) Blomley, M. J., Cooke, J. C., Unger, E. C., Monaghan, M. J., and Cosgrove, D. O. (2001) Microbubble contrast agents: a new era in ultrasound. *BMJ* 322, 1222–1225.

(17) Klibanov, A. L. (2006) Microbubble contrast agents: targeted ultrasound imaging and ultrasound-assisted drug-delivery applications. *Invest. Radiol.* 41, 354–362.

(18) Jain, R. K., and Stylianopoulos, T. (2010) Delivering nanomedicine to solid tumors. *Nat. Rev. Clin. Oncol.* 7, 653–664.

(19) Fang, J., Nakamura, H., and Maeda, H. (2011) The EPR effect: Unique features of tumor blood vessels for drug delivery, factors involved, and limitations and augmentation of the effect. *Adv. Drug Delivery Rev.* 63, 136–151.

(20) Nakamura, Y., Mochida, A., Choyke, P. L., and Kobayashi, H. (2016) Nanodrug Delivery: Is the Enhanced Permeability and Retention Effect Sufficient for Curing Cancer? *Bioconjugate Chem.* 27, 2225–2238.

(21) Yang, S., Wang, P., Wang, X. B., Su, X. M., and Liu, Q. H. (2014) Activation of microbubbles by low-level therapeutic ultrasound enhances the antitumor effects of doxorubicin. *European Radiology* 24, 2739–2753.

(22) Huynh, E., Leung, B. Y. C., Helfield, B. L., Shakiba, M., Gandier, J.-A., Jin, C. S., Master, E. R., Wilson, B. C., Goertz, D. E., and Zheng, G. (2015) *Nat. Nanotechnol.* 10, 325.

(23) Huynh, E., Lovell, J. F., Helfield, B. L., Jeon, M., Kim, C., Goertz, D. E., Wilson, B. C., and Zheng, G. (2012) Porphyrin shell microbubbles with intrinsic ultrasound and photoacoustic properties. *J. Am. Chem. Soc.* 134, 16464–16467.

(24) Nomikou, N., Fowley, C., Byrne, N. M., McCaughan, B., McHale, A. P., and Callan, J. F. (2012) Microbubble-sonosensitizer conjugates as therapeutics in sonodynamic therapy. *Chem. Commun.* 48, 8332–8334.

(25) McEwan, C., Owen, J., Stride, E., Fowley, C., Nesbitt, H., Cochrane, D., Coussios, C. C., Borden, M., Nomikou, N., McHale, A. P., et al. (2015) Oxygen carrying microbubbles for enhanced sonodynamic therapy of hypoxic tumours. *J. Controlled Release* 203, 51–56.

(26) Wang, H. P., Wang, P., Li, L., Zhang, K., Wang, X. B., and Liu, Q. H. (2015) Microbubbles Enhance the Antitumor Effects of Sinoporphyrin Sodium Mediated Sonodynamic Therapy both In Vitro and In Vivo. *Int. J. Biol. Sci.* 11, 1401–1409.

(27) Liu, Y., Wan, G., Guo, H., Liu, Y., Zhou, P., Wang, H., Wang, D., Zhang, S., Wang, Y., and Zhang, N. (2017) A multifunctional nanoparticle system combines sonodynamic therapy and chemo-therapy to treat hepatocellular carcinoma. *Nano Res.* 10, 834–855.

(28) Perera, R. H., Hernandez, C., Zhou, H. Y., Kota, P., Burke, A., and Exner, A. A. (2015) Ultrasound imaging beyond the vasculature with new generation contrast agents. *Wiley Interdisciplinary Reviews- Nanomedicine and Nanobiotechnology* 7, 593–608.

(29) Wu, H. P., Roguin, N. G., Krupka, T. M., Solorio, L., Yoshiara, H., Guenette, G., Sanders, C., Kamiyama, N., and Exner, A. A. (2013) Acoustic Characterization and Pharmacokinetic Analyses of New Nanobubble Ultrasound Contrast Agents. *Ultrasound in Medicine and Biology* 39, 2137–2146.

(30) Perera, R. H., Wu, H. P., Peiris, P., Hernandez, C., Burke, A., Zhang, H., and Exner, A. A. (2017) Improving performance of nanoscale ultrasound contrast agents using N,N-diethylacrylamide stabilization. *Nanomedicine* 13, 59–67

(31) Krupka, T. M., Solorio, L., Wilson, R. E., Wu, H., Azar, N., and Exner, A. A. (2010) Formulation and Characterization of Echogenic Lipid-Pluronic Nanobubbles. *Mol. Pharmaceutics* 7, 49–59.

(32) Perera, R. H., Solorio, L., Wu, H., Gangolli, M., Silverman, E., Hernandez, C., Peiris, P. M., Broome, A.-M., and Exner, A. A. (2014) Nanobubble Ultrasound Contrast Agents for Enhanced Delivery of Thermal Sensitizer to Tumors Undergoing Radiofrequency Ablation. *Pharm. Res.* 31, 1407–1417.

(33) Janib, S. M., Moses, A. S., and MacKay, J. A. (2010) Imaging and drug delivery using theranostic nanoparticles. *Adv. Drug Delivery Rev.* 62, 1052–1063.

(34) Mikata, Y., Sawaguchi, T., Kakuchi, T., Gottschaldt, M., Schubert, U. S., Ohi, H., and Yano, S. (2010) Control of the Aggregation

Properties of Tris(maltohexaose)-Linked Porphyrins with an Alkyl Chain. *Eur. J. Org. Chem.* 2010, 663–671.

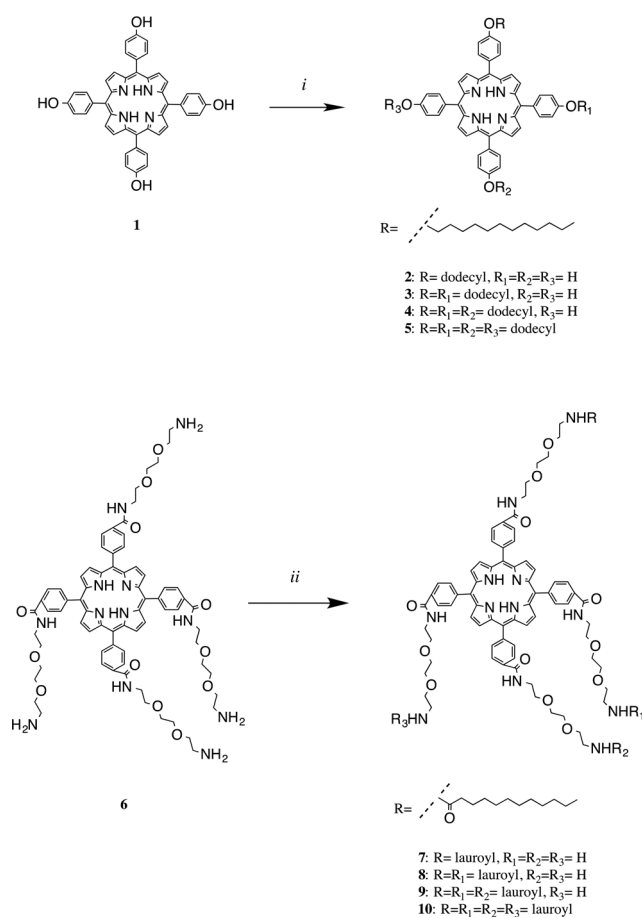
(35) Bosca, F., Orio, L., Tagliapietra, S., Corazzari, I., Turci, F., Martina, K., Pastero, L., Cravotto, G., and Barge, A. (2016) Microwave-Assisted Synthesis and Physicochemical Characterization of Tetrafuranylporphyrin-Grafted Reduced-Graphene Oxide. *Chem. - Eur. J.* 22, 1608–1613.

(36) Hernandez, C., Gulati, S., Fioravanti, G., Stewart, P. L., and Exner, A. A. (2017) Cryo-EM Visualization of Lipid and Polymer-Stabilized Perfluorocarbon Gas Nanobubbles - A Step Towards Nanobubble Mediated Drug Delivery. *Sci. Rep.* 7, 13517.

(37) Qian, X., Zheng, Y., and Chen, Y. (2016) Micro/Nanoparticle-Augmented Sonodynamic Therapy (SDT): Breaking the Depth Shallow of Photoactivation. *Adv. Mater.* 28, 8097–8129.

(38) Wan, G.-Y., Liu, Y., Chen, B.-W., Liu, Y.-Y., Wang, Y.-S., and Zhang, N. (2016) Recent advances of sonodynamic therapy in cancer treatment. *Cancer Biol. Med.* 13, 325–338.

Scheme 1. Synthetic Pathway of Compounds 2–5 and 7–10<sup>a</sup>



<sup>a</sup>Synthetic pathway of compounds 2–5: (i) Meso-tetrakis-(4-hydroxyphenyl)-porphyrin (1, commercial available), 1-Bromododecane in CH<sub>2</sub>Cl<sub>2</sub>, DMF, Na<sub>2</sub>CO<sub>3</sub>, and 18-crown-6 (catalytic amount). Synthetic pathway of compounds 7–10: (ii) Meso-tetrakis-[4-(aminoethoxyethoxyethylaminocarbonyl)-phenyl]-porphyrin (compound 6), lauryl chloride in CH<sub>3</sub>CN, Dioxane and CH<sub>3</sub>CN, Na<sub>2</sub>CO<sub>3</sub>.

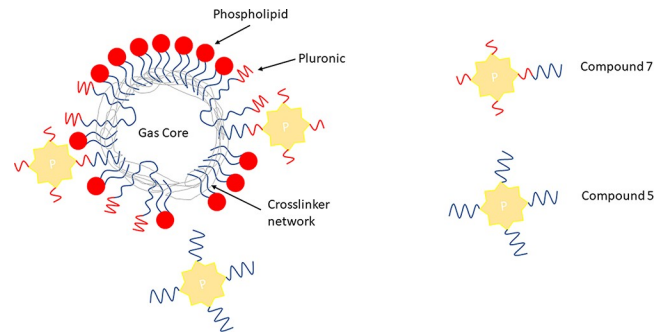


Figure 1. Design of porphyrin loaded NB. Porphyrin compound 7 shows a red line indicating amphiphilic chain structure and blue line indicating lipophilic chain. For porphyrin compound 5, only blue lines (lipophilic chain) are present.

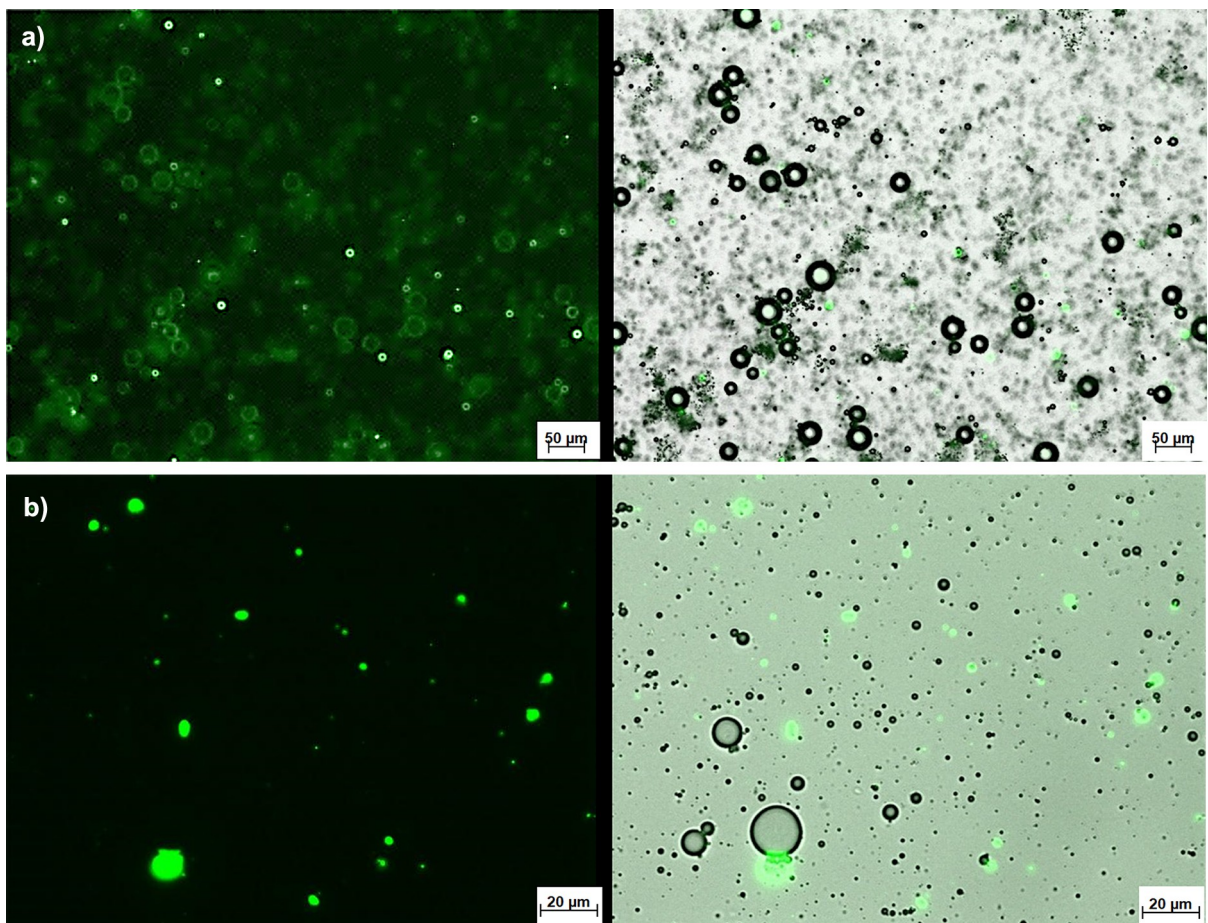


Figure 2. (A) Fluorescent microscopy of amphiphilic compound 7-NBs (20 $\times$ , 50  $\mu\text{m}$  scale bar). The picture on the right is an overlay of the fluorescent image (shown on the left) and a bright field image to visualize porphyrin incorporation into the lipid bubble. (B) Fluorescent microscopy of lipophilic compound 5-NBs (40 $\times$ , 20  $\mu\text{m}$  scale bar). The picture on the right is an overlay of the fluorescent image (shown on the left) and a bright field image to visualize porphyrin incorporation into the lipid bubble.

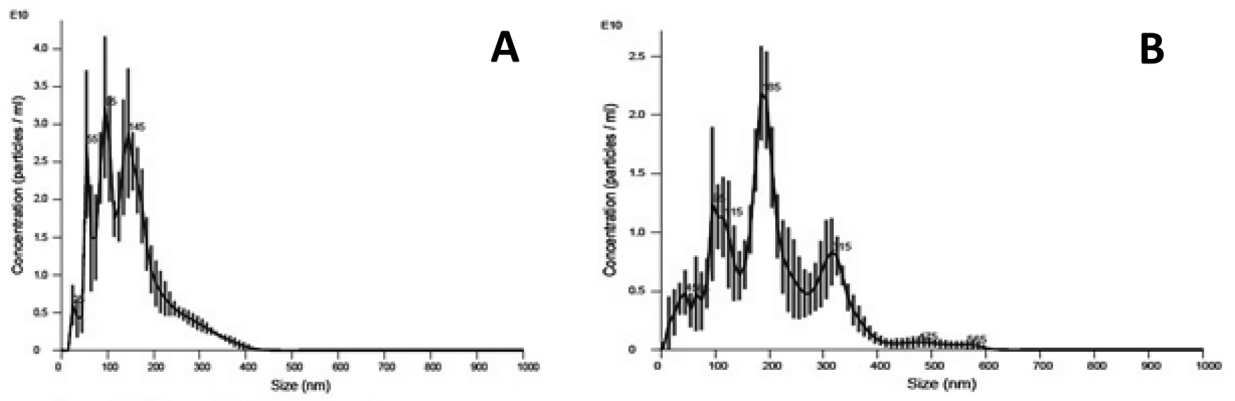


Figure 3. Diameter (nm) distribution of the porphyrin-loaded NBs obtained by nanoparticle tracking analysis (NanoSight, Malvern Instruments): compound 7-NBs (A) and compound 5-NBs (B) trend

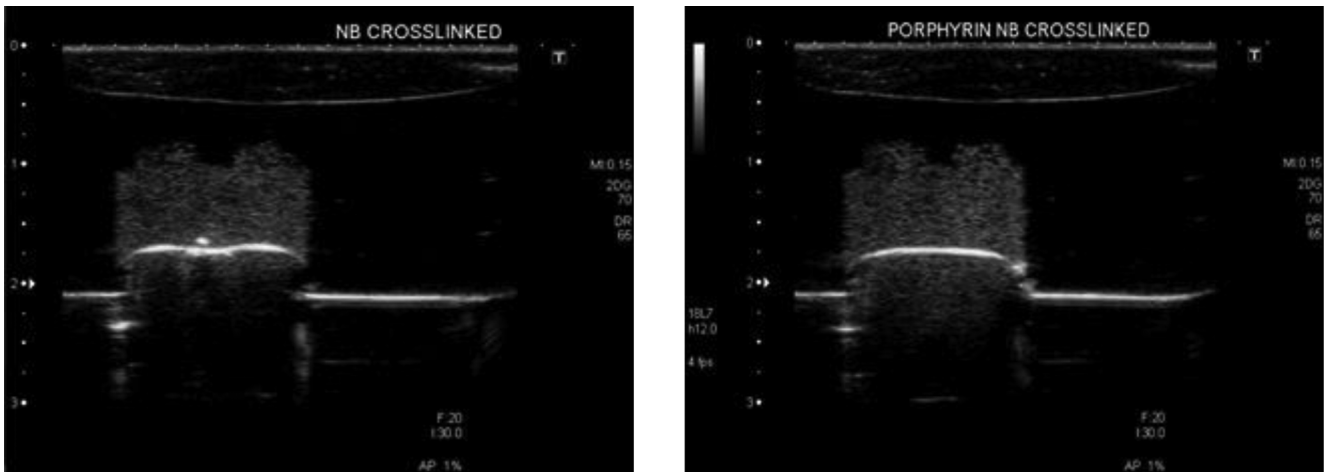


Figure 4. Representative ultrasound images of nanobubbles: unloaded NBs (left) and compound 7-loaded NBs (right). Images are shown inverted due to transducer orientation. Ultrasound images were acquired with contrast harmonic imaging at 12 MHz and MI of 0.15 (calculated pressure at the beam focus = 231.54 KPa).



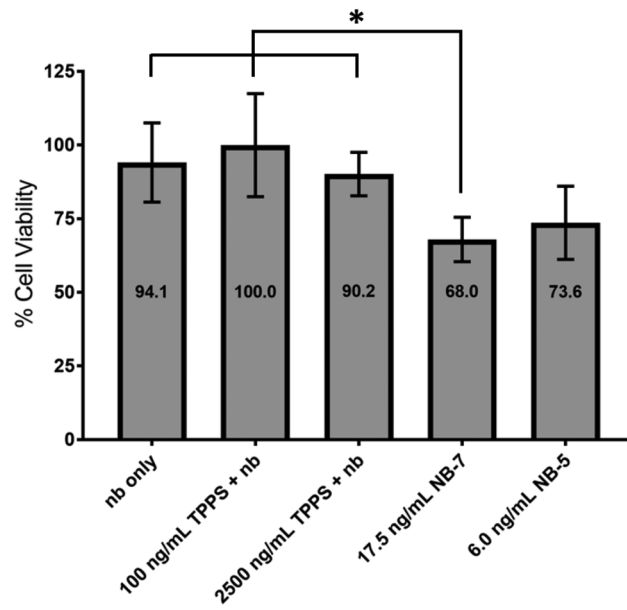


Figure 5. *In vitro* test on LS 174 T cell line (human colon adenocarcinoma) US irradiated for 3 min using 20% duty cycle, 3 MHz transducer, 1.8 W/cm<sup>2</sup> intensity. Studies were carried out under temperature controlled conditions (37 °C). Loaded NB: NB-7, total porphyrin content of 17.5 ng/mL; NB-5, total porphyrin content of

6.0 ng/mL. NB particle concentration was kept constant for all wells. "nb" indicates unloaded nanobubbles. \* indicates  $p < 0.05$  as determined by a Student's *t* test.